

1992-11-17

1193-18924

140087

P. 8

# A Statistical Model for Evaluating GOPEX Uplink Performance

K. Kiesaleh and T.-Y. Yan  
Communications Systems Research Section

*This article describes a statistical model to analyze the signal intensity received at the solid-state imaging (SSI) camera of the Galileo optical communications system from an Earth-based transmitter (GOPEX) demonstration. The analytical model assumes that the optical beam possesses a Gaussian profile and the communication channel has a log-normal scattering characteristic. The atmospheric-induced jitter is modelled as two independent zero mean Gaussian random variables. By modelling the system parameters as a set of independent and identically distributed (iid) random variables, the combined impact of uncertainties due to system parameters and the turbulent atmosphere can be approximated by a log-normal distributed signal intensity at the spacecraft. A Monte-Carlo software simulation package has also been developed to compute the confidence interval probabilities for general optical beam profiles. Numerical results show that the approximation is valid for a wide range of operation scenarios.*

## I. Introduction

In this article, analytical expressions for the probability density functions (pdf's) of the optical field intensity and the number of observed photoelectrons per pixel of Galileo's solid-state camera for a laser pulse interval in the Galileo optical communication from an Earth-based transmitter (GOPEX) experiment are derived. These pdf's play a critical role in assessing the performance of this optical uplink and provide a means of acquiring meaningful design predicts. Furthermore, the aforementioned pdf's shed light on the characteristics of the underlying processes involved

in this experiment and the impacts of various parameters on the detection probability.

It is assumed that the main sources of disturbance are the atmosphere-induced jitter, for the short-exposure model at hand, and the log-normal large-particle channel scattering, which proves to be significant for the operating characteristics of this experiment. In general, there are a number of parameters, described below, that directly impact the observed signal intensity at the spacecraft. These parameters are assumed to be independent and identically

distributed (iid) random variables. It is imperative to note the importance of this observation, since as a result of this assumption the signal intensity in the absence of atmospheric effects may be approximated by a log-normal random variable as well. In this article, the log-normal channel scattering is shown to be the dominant effect for the operating characteristics of this experiment. Thus, it is concluded that the combined impact of random system parameters and turbulent atmosphere would yield a log-normal distributed signal intensity at the spacecraft. Before going any further, a description of the system parameters that directly impact the observed signal intensity and which are needed to conduct the ensuing analytical study of the GOPEX uplink is presented.

The optical field intensity at the spacecraft is a function of transmitter optics efficiency,  $\eta_t$ , receiver optics efficiency,  $\eta_r$ , atmospheric transmittance,  $\eta_{atm}$ , transmitter laser energy (in joules),  $W_t$ , distance from the spacecraft,  $Z$ , and the predefined angular beam diameter,  $\theta_s$ . Since the number of photoelectrons per pixel, observed over a laser pulse duration, is of importance here, one must also include the effective detector area (pixel area),  $A_{rec}$ , and the quantum efficiency of the photodetector,  $\eta_c$ , in determining the overall statistical modelling. In the event of a uniform beam pattern, and for  $Z \gg 1$ , one can describe the optical field intensity in joules/m<sup>2</sup> at the spacecraft as

$$\langle I(x, y, t) \rangle_t = \frac{4W_t}{\pi Z^2 \theta_s^2} \eta_t \eta_r \eta_{atm} \quad (1)$$

where  $\langle I(x, y, t) \rangle_t$  describes the intensity in the plane of observation at coordinates  $(x, y)$ , and  $\langle \cdot \rangle_t$  signifies short-term intensity averaging over time, since the observation interval is limited to only 6 to 12 nsec, the laser pulse duration. The number of observed photoelectrons in the laser pulse duration is then

$$N_{electron} = \langle I(x, y, t) \rangle_t A_{rec} \eta_c \quad (2)$$

These expressions will be modified in the next section to include the Gaussian beam profile and the log-normal large-particle scattering effect.

## II. Uplink Analysis: Gaussian Beam Profile

In this section, a transmitted beam with a Gaussian profile is assumed. Therefore, for a short exposure model, one may assume that the Gaussian beam profile maintains its integrity in the plane of observation. In this case, the

optical field intensity at  $(x, y)$  in the plane of observation may be approximated by

$$\langle I(x, y, t) \rangle_t \approx \frac{4W_t}{\pi Z^2 \theta_s^2} \eta_t \eta_r \eta_0^{\sec(\theta)} I_l \exp \left[ -\frac{4(x^2 + y^2)}{\theta_s^2 Z^2} \right] \quad (3)$$

where now  $I_l$  accounts for the log-normal atmospheric scattering effect,  $\eta_0$  is the atmospheric loss at zenith, and  $\theta$  is the spacecraft's zenith angle. This implies that  $\eta_{atm} = \eta_0^{\sec(\theta)}$ , which agrees with most experimental and theoretical studies of atmospheric absorption. In this analysis, assume a negligible pointing error, and thus the field intensity must be evaluated for  $(x, y) = (0, 0)$ . Furthermore, since the receiving area of the charged-coupled device (CCD) camera is significantly smaller than the beam footprint at the spacecraft location, the CCD camera may be considered a point detector. Therefore, Eq. (3) at  $(x, y) = (0, 0)$  accurately describes the field intensity for all the detectors of the CCD camera.

The pdf of  $I_l$  is given by the well-known log-normal density

$$f_{I_l}(i_l) = \frac{1}{\sqrt{2\pi\sigma_l^2} i_l} \times \exp \left\{ -\frac{[\ln(i_l) + \frac{\sigma_l^2}{2}]^2}{2\sigma_l^2} \right\}; \quad i_l \geq 0 \quad (4)$$

where  $\sigma_l$  is, in turn, given by [1]

$$\sigma_l^2 \approx 2.24 \left( \frac{2\pi}{\lambda} \right)^{\frac{7}{8}} \sec(\theta)^{\frac{11}{8}} \times \int_0^H C_n^2(h) h^{\frac{5}{8}} dh \quad (5)$$

In the above equation,  $\lambda$  is the wavelength of the laser in meters,  $H$  is the height of the atmosphere, and  $C_n(h)$  is the medium index of the refraction structure constant. Major stumbling blocks in determining an accurate estimate of  $\sigma_l^2$  are the dependency of  $C_n$  on various random channel parameters and the unavailability of an accurate model for  $C_n$ . However, in the literature a number of approximate models for this structure constant are available.

For a complete list, refer to [2]. Among those references, the following expression, originally proposed by Hufnagel, approximates this structure constant:

$$C_n^2(h) = 8.2 \times 10^{-56} V^2 h^{10} e^{-h/1000} + 2.7 \times 10^{-16} e^{-h/1500} \quad (6)$$

where  $h$  is the altitude in meters above sea level and  $V$  is the rms wind velocity, averaged over 5 to 20 km altitude, and is considered to be Gaussian distributed about a mean of 27 m/sec with a standard deviation of 9 m/sec. This model, however, is valid only for altitudes in excess of 5 km. For altitudes below 5 km, an approximate expression from Hufnagel and Stanely for the structure constant is given by

$$C_n^2(h) \approx 1.5 \times 10^{-13}/h \quad (7)$$

For the parameters of the GOPEX project, and based upon the above approximations,  $\sigma_l \leq 0.9$ .

In a turbulent medium, a Gaussian beam, as described above, experiences deflection in various directions due to gaseous blobs and other turbulent particles flowing through the path of the beam. For a short exposure model (6- to 12-nsec observation interval), the atmospherically induced deflections may accurately be modelled as atmospherically induced pointing "jitter." This implies that  $x$  and  $y$  in Eq. (3) may now be viewed as two independent and zero mean Gaussian random variables with standard deviation  $\sigma Z$ . Thus,  $\sigma$  represents the rms angular (half-beam) jitter due to turbulence. When pointing error is present, its standard deviation may be added directly to  $\sigma$ . However, caution must be exercised in applying the ensuing results to a model with a constant pointing error. In this event,  $x$  and  $y$  are nonzero mean Gaussian random variables. For this analysis, however, the constant pointing error is considered to be negligible, and thus one may consider  $x$  and  $y$  as zero mean Gaussian random variables.

The standard deviation  $\sigma$  can be estimated for a given index of refraction profile by using the following expression [3]:

$$\sigma = \frac{2}{k} \left[ 1.46 k^2 \sec(\theta) \times \int_0^{20000} d\zeta C_n^2(\zeta) \left(1 - \frac{\zeta}{20000}\right)^{5/3} \right]^{3/5} \quad (8)$$

where  $k$  is the wave number. For the parameters of this experiment,  $\sigma$  is estimated to be 9  $\mu$ rad for near zenith and 14  $\mu$ rad for a zenith angle of 60 deg. Define the random variable  $I_g$  as follows:

$$I_g(x, y) = \exp \left[ -\frac{4(x^2 + y^2)}{\theta_s^2 Z^2} \right] \quad (9)$$

It can readily be shown that for jointly Gaussian  $x$  and  $y$ ,  $I_g$  is a special case of beta distributed random variables with pdf

$$f_{I_g}(i_g) = \beta i_g^{\beta-1}; \quad 0 \leq i_g \leq 1 \quad (10)$$

where  $\beta = \theta_s^2/8\sigma^2$ . In the following,  $\beta$  ranges from 5 to 19 ( $\theta_s = 110 \mu$ rad and  $\sigma \approx 9$  to 14  $\mu$ rad) for all practical purposes. It is interesting to note that for  $\beta = 1$  this density reduces to a uniform density, signifying the detrimental impact of a turbulent medium.

The pdf of  $I_t = I_g I_l$  can now be found. It represents the combined impact of log-normal medium scattering and atmospherically induced pointing jitter. This pdf is expressed as

$$f_{I_t}(i_t) = \beta \exp \left[ \frac{\sigma_l^2}{2} \beta(\beta + 1) \right] i_t^{\beta-1} \times Q \left[ \frac{\ln(i_t) + \sigma_l^2(\beta + 1/2)}{\sigma_l} \right]; \quad I_t \geq 0 \quad (11)$$

where  $Q(x) = 1/(\sqrt{2\pi}) \int_x^\infty \exp(-s^2/2) ds$ . For a reasonable range of system parameters, this density is depicted in Figs. 1 through 4. It is important to note that  $\sigma_l$  plays a critical role in determining the behavior of this random variable. Unfortunately, for zenith angles in the range of 40 to 55 deg,  $\lambda = 0.532 \mu$ m, and a rms wind velocity of 27 m/s,  $\sigma_l$  proves to be in excess of 0.2, resulting in a pdf that can accurately be approximated by a log-normal density function. This implies that for all practical purposes,

$$f_{I_t}(i_t) \approx \frac{1}{\sqrt{2\pi\sigma_l^2 i_t}} \times \exp \left\{ -\frac{[\ln(i_t) - m_t]^2}{2\sigma_l^2} \right\}; \quad i_t \geq 0 \quad (12)$$

where

$$m_i = \int_0^\infty \ln(s) \beta \exp\left[\frac{\sigma_i^2}{2}\beta(\beta+1)\right] s^{(\beta-1)} \times Q\left[\frac{\ln(s) + \sigma_i^2(\beta+1/2)}{\sigma_i}\right] ds \quad (13)$$

$$\sigma_i^2 = \int_0^\infty \ln^2(s) \beta \exp\left[\frac{\sigma_i^2}{2}\beta(\beta+1)\right] s^{(\beta-1)} \times Q\left[\frac{\ln(s) + \sigma_i^2(\beta+1/2)}{\sigma_i}\right] ds - m_i^2 \quad (14)$$

These expressions can be numerically evaluated for a desired set of system parameters. The validity of approximating the characteristics of  $I_t$  with that of a log-normal random variable is examined in a number of plots (see Figs. 5 through 8). As noted, for a wide range of system parameters the penalty for this approximation is comfortably small.

One can now express the number of observed photoelectrons in a pulse interval as

$$N_{electron} = \frac{4W_t}{\pi Z^2 \theta_s^2} \eta_{tot} I_t \quad (15)$$

where  $\eta_{tot} = \prod_{i=1}^5 \eta_i$ , with  $\eta_1 = \eta_r$ ,  $\eta_2 = \eta_t$ ,  $\eta_3 = \eta_0^{\sec(\theta)}$ ,  $\eta_4 = \eta_c$ , and  $\eta_5 = A_{rec}$ . If one considers  $\eta_i$ 's as iid random variables, it is possible to approximate  $\eta_{tot}$  with a log-normal random variable. Due to a lack of sufficient data for accurate characterization of these parameters or for considering the worst-case scenario, one may assume that  $\eta_i$  is uniform over  $(\eta_i^{min}, \eta_i^{max})$  for all  $i$ . In this event,

$$f_{\eta_{tot}}(\eta_{tot}) \approx \frac{1}{\sqrt{2\pi\sigma_\eta^2\eta_{tot}}} \times \exp\left\{-\frac{[\ln(\eta_{tot}) - m_\eta]^2}{2\sigma_\eta^2}\right\}; \eta_{tot} \geq 0 \quad (16)$$

where  $m_\eta = \sum_{i=1}^5 m_{\eta_i}$ , and  $\sigma_\eta^2 = \sum_{i=1}^5 \sigma_{\eta_i}^2$ , with

$$m_{\eta_i} = \frac{1}{\eta_i^{max} - \eta_i^{min}} \int_{\eta_i^{min}}^{\eta_i^{max}} \ln(s) ds = \frac{1}{\eta_i^{max} - \eta_i^{min}}$$

$$\times [\eta_i^{max} \ln(\eta_i^{max}) - \eta_i^{min} \ln(\eta_i^{min})] - 1 \quad (17)$$

$$\sigma_{\eta_i}^2 = \frac{\eta_i^{max}}{\eta_i^{max} - \eta_i^{min}} \times \left[ \ln^2(\eta_i^{max}) - 2 \ln\left(\frac{\eta_i^{max}}{e}\right) \right] - \frac{\eta_i^{min}}{\eta_i^{max} - \eta_i^{min}} \times \left[ \ln^2(\eta_i^{min}) - 2 \ln\left(\frac{\eta_i^{min}}{e}\right) \right] - m_{\eta_i}^2 \quad (18)$$

Because the product of two log-normal random variables yields log-normal statistics

$$f_{N_{tot}}(n_{tot}) \approx \frac{1}{\sqrt{2\pi\sigma_N^2 n_{tot}}} \times \exp\left\{-\frac{[\ln(n_{tot}) - m_N]^2}{2\sigma_N^2}\right\}; n_{tot} \geq 0 \quad (19)$$

where  $N_{tot} = \eta_{tot} I_t$ ,  $m_N = m_\eta + m_t$ , and  $\sigma_N^2 = \sigma_\eta^2 + \sigma_t^2$ . Finally, the total number of photoelectrons observed over a pulse interval is given by

$$N_{electron} = \frac{4W_t}{\pi Z^2 \theta_s^2} N_{tot} \quad (20)$$

Note that an alternate means of computing  $\sigma_N$  and  $m_N$  is to first compute the mean and mean-square of  $\eta_{tot} I_t$ , which are given by

$$E\{N_{tot}\} = \frac{\beta}{1+\beta} \prod_{i=1}^5 \frac{(\eta_i^{max} + \eta_i^{min})}{2} \quad (21)$$

$$E\{N_{tot}^2\} = \exp(\sigma_t^2) \frac{\beta}{2+\beta} \times \prod_{i=1}^5 \frac{[(\eta_i^{max})^2 + (\eta_i^{min})^2 + \eta_i^{max} \eta_i^{min}]}{3} \quad (22)$$

and use the following expressions:

$$\sigma_N^2 = \log [E\{N_{tot}^2\}/E^2\{N_{tot}\} + 1] \quad (23)$$

$$m_N = \log [E\{N_{tot}\}] - \frac{1}{2}\sigma_N^2 \quad (24)$$

It is imperative to note that the accuracy of the above model is highly sensitive to  $\sigma_l$  and other system parameters. In particular, caution must be exercised in assuming a log-normal scattering model for values of  $\sigma_l > 0.75$ , since for such values of  $\sigma_l$  the variance of the normalized intensity fluctuation due to scattering (i.e.,  $e^{\sigma_l^2} - 1$ ) exceeds 0.75. In this event, log-normal statistics are no longer valid in describing the characteristics of the scattering channel. Instead, an exponential pdf must be employed to characterize the scattering channel [3,4]. For the experiment at hand,  $\sigma_l$  for  $V \leq 27$  m/sec and  $\theta \leq 55$  deg is less than 0.9. This, therefore, makes the log-normal assumption rather suspect for some portion of this experiment where the spacecraft takes on large zenith angles. However, since the rms wind velocity is a random variable, and  $\sigma_l$  is highly sensitive to this parameter, one may approximate the channel scattering effect with the log-normal statistic.

### III. Uplink Analysis: General Beam Profile

This section provides a brief description of a software simulation package that was developed for the analysis of the GOPEX uplink when the optical beam possesses a general profile. To compute confidence interval probabilities, one has to resort to a Monte Carlo simulation to include the impacts of atmospherically induced jitter, log-normal channel scattering, and uncertainties in other system parameters that are modelled as uniformly distributed random variables (see above).

This package reads the beam matrix profile, recorded at a known distance, and evaluates the beam profile at the location of the spacecraft. The turbulent medium is, once again, modelled as a zero mean Gaussian pointing jitter in both  $x$  and  $y$  coordinates. This program provides the mean, standard deviation, and the pdf of the number of observed photoelectrons in a pulse duration for a specified interval. The confidence probability for a given confidence interval is also computed. Since no theoretical results were available to test the validity of the results

of this program for a general beam profile, a Gaussian beam was specified as the input beam profile. The system parameters were set at the following values:  $W_t = 0.25$  joules,  $\lambda = 0.532 \mu\text{m}$ ,  $\theta_s = 110 \mu\text{rad}$ ,  $\eta_t = 0.705$ ,  $\eta_r = 0.24$ ,  $\eta_c = 0.37$ ,  $\eta_0 = 0.715$  (atmospheric attenuation at zenith and station altitude of 2.286 km [5]),  $A_{rec} = 0.01825 \text{ m}^2$ ,  $Z = 0.6 \times 10^6 \text{ km}$ ,  $V = 27 \text{ m/sec}$ , and  $\theta = 55 \text{ deg}$ . From the above analytical results for the Gaussian beam profile, the mean and standard deviation of the observed photoelectrons were estimated at  $111.991 \times 10^3$  and  $126.08 \times 10^3$ , respectively. The large standard deviation is a clear indication of log-normal statistics due to dominant channel scattering. The simulation for 10,000 samples yielded the following mean and standard deviation:  $110.834 \times 10^3$  and  $119.535 \times 10^3$ . These numbers improved to  $111.950 \times 10^3$  and  $124.361 \times 10^3$  for 50,000 samples. It is quite clear that a reasonable accuracy may be achieved with a relatively small number of samples. However, with the aid of stratified or importance sampling, the required number of samples may be drastically reduced. The above calculation was repeated for a 60-deg elevation, i.e.,  $\theta = 30 \text{ deg}$ , with the remaining parameters fixed at the above values. From theoretical results, the mean and standard deviation were found to be  $142.025 \times 10^3$  and  $97.166 \times 10^3$ , respectively. For 10,000 samples, simulation yielded  $141.27 \times 10^3$  and  $94.877 \times 10^3$  as the mean and standard deviation of the observed photoelectrons, respectively. Once again, these numbers improved to  $142.095 \times 10^3$  and  $96.536 \times 10^3$  for 50,000 samples, clearly indicating the consistency of the simulation.

### IV. Conclusion

This article described a statistical model to evaluate the signal intensity received at the solid-state imaging camera for the GOPEX demonstration. The model includes the effect of log-normal channel scattering, atmospherically induced jitter, and uncertain system parameters. It has been shown that the resulting probability density function can be well approximated by a log-normal distribution. A Monte Carlo simulation software package has been developed to analyze the uplink performance when the optical beam profile is non-Gaussian. The confidence-interval probability can be computed to analyze the GOPEX experimental data during demonstration.

## References

- [1] V. I. Tatarskii, *Wave Propagation in a Turbulent Medium*, New York: McGraw Hill, 1961.
- [2] W. L. Wolf and G. J. Zisis, Chapter 6 in *The Infrared Handbook*, Detroit: The Infrared Information Analysis (IRIA) Center, Environmental Research Institute of Michigan, 1989.
- [3] S. Karp, R. Gagliardi, S. E. Moran, and L. B. Stotts, *Optical Channels*, New York: Plenum Press, pp. 178–180, 1988.
- [4] R. Fante, Electromagnetic Beam Propagation in Turbulent Medium, an Update, *Proc. IEEE*, vol. 68, pp. 1424–1443, 1980.
- [5] K. S. Shaik, “Atmospheric Transmission Calculations for Optical Frequencies,” *Proceedings of the Thirteenth NASA Propagation Experiments Meeting (NAPEX XIII)*, pp. 158–162, June 29–30, 1989.

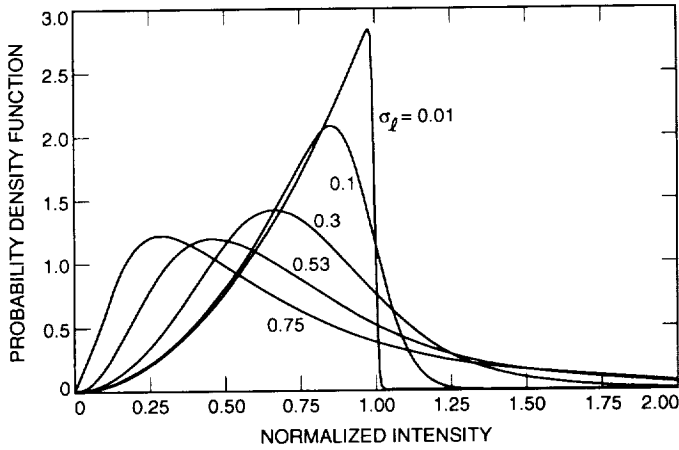


Fig. 1. Probability density function of the normalized intensity,  $\beta = 3$ .

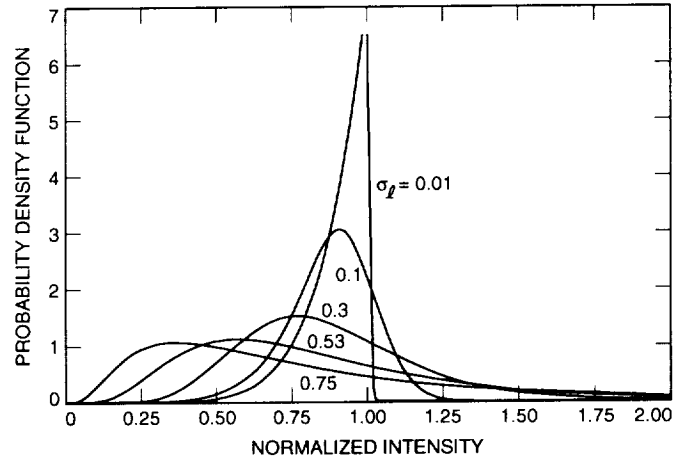


Fig. 3. Probability density function of the normalized intensity,  $\beta = 7$ .

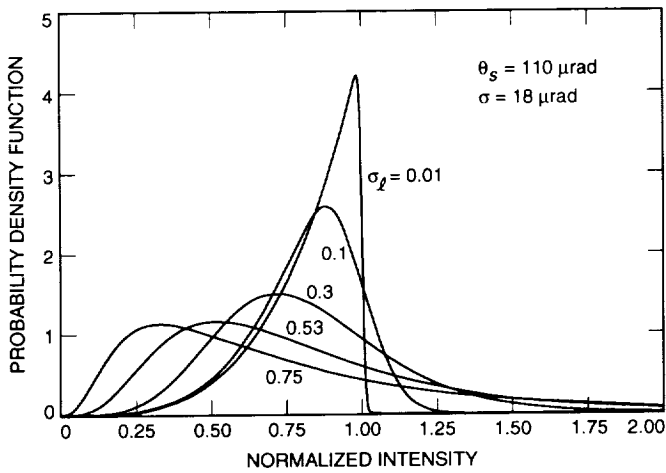


Fig. 2. Probability density function of the normalized intensity,  $\beta = 4.6$ .

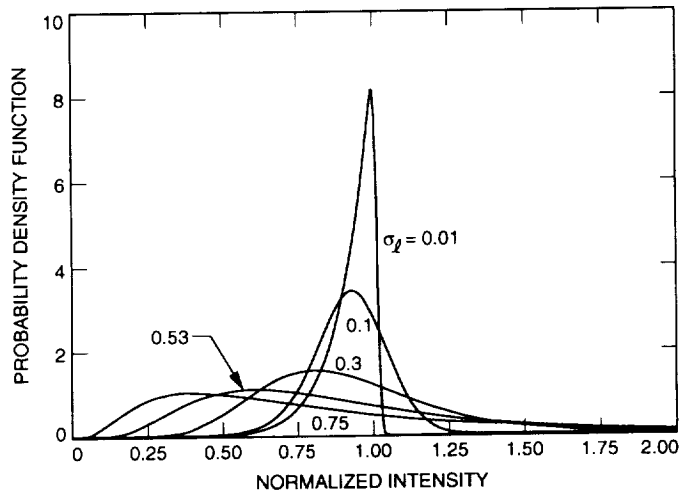


Fig. 4. Probability density function of the normalized intensity,  $\beta = 10$ .

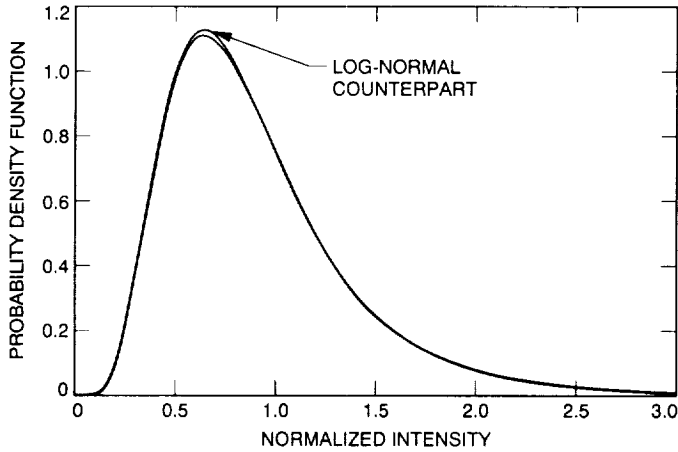


Fig. 5. Probability density function of the normalized intensity,  $\beta = 5$  and  $\sigma_\ell = 0.5$ , and its approximated log-normal counterpart.

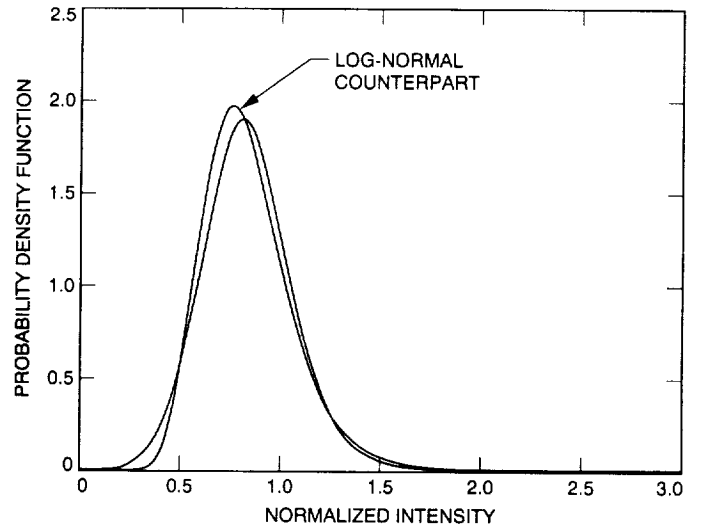


Fig. 7. Probability density function of the normalized intensity,  $\beta = 5$  and  $\sigma_\ell = 0.2$ , and its approximated log-normal counterpart.

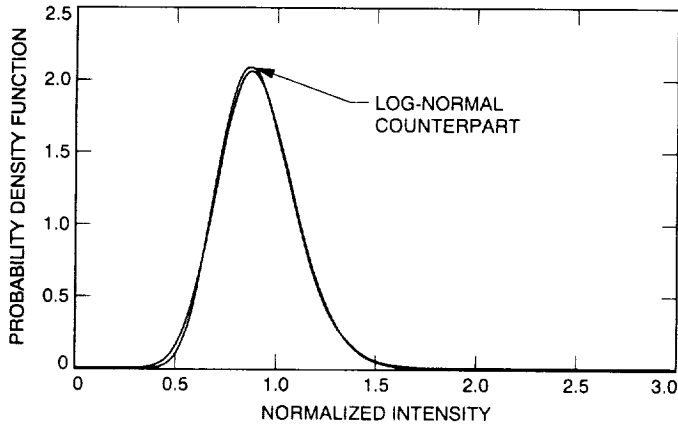


Fig. 6. Probability density function of the normalized intensity,  $\beta = 10$  and  $\sigma_\ell = 0.2$ , and its approximated log-normal counterpart.

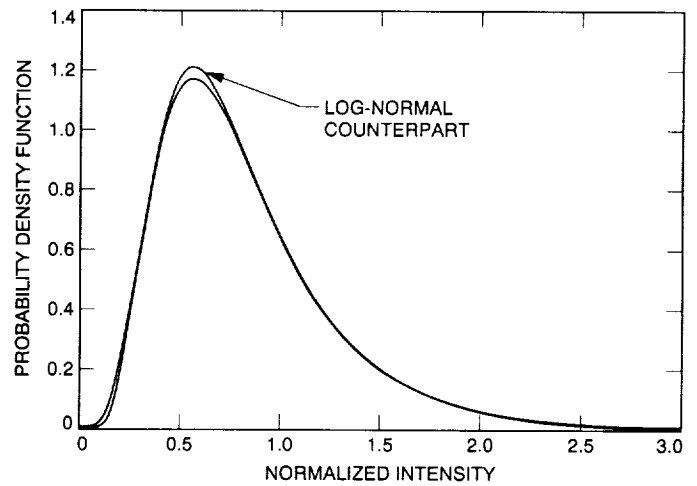


Fig. 8. Probability density function of the normalized intensity,  $\beta = 5$  and  $\sigma_\ell = 0.5$ , and its approximated log-normal counterpart.